Inorg. Chem. **2008**, *47*, 4808−4816

Redox Active Cage for the Electrochemical Sensing of Anions

Valeria Amendola,[†] Massimo Boiocchi,[‡] Benoît Colasson,[§,⊥] Luigi Fabbrizzi,[*,†] Enrico Monzani,[†] Maria Jesús Douton-Rodriguez,[†] and Cristina Spadini[†]

Dipartimento di Chimica Generale, Sezione INSTM, and Centro Grandi Strumenti, Università di Pavia, 27100, Pavia, Italy

Received January 18, 2008

The tripodal system $[\mathbf{1}]^{3+}$ forms a 1:1 complex with Co^{II} in which the metal is octahedrally coordinated by three bpy fragments. The $[Co^{II}(\mathbf{1})]^{5+}$ complex provides a cavity suitable for solvent or anion inclusion. X-ray diffraction studies on the crystalline complex salt of formula $[Co^{II}(\mathbf{1})\cdots H_2O]Cl(PF_6)_4\cdot 2MeCN$ have shown that a water molecule is included in the cavity and the water oxygen atom receives six H-bonds from the C−H fragments of the three imidazolium subunits and of the three proximate pyridine rings, according to a slightly distorted trigonal prismatic geometry. Anion inclusion in an aqueous MeCN solution induces a distinct cathodic shift of the potential of the Co^{III}/Co^{II} couple, whose magnitude decreases along the series: $Cl^- > Br^- \sim NCO^- > I^- \sim NCS^-$, which reflects anion tendencies to receive H-bonds from the receptor. The variation of the water content in the MeCN solution (from 0 to 20%) induces a gradual change of the voltammetric response to anion titration: from two well distinguished peaks at a fixed potential to a single peak progressively shifted to a more cathodic potential. Such a behavior parallels the gradual decrease of the equilibrium constant for anion inclusion into the $[Co^{II}(\mathbf{1})]^{5+}$ receptor.

Introduction

The design of selective receptors for inorganic anions is inescapably more elaborated than that of ligands for metal ions.[1] In fact, anions establish rather weak interactions with receptors, electrostatic or hydrogen bonding, and, to form solution stable complexes, they need to profit from a high level of preorganization of the receptor.[2] In particular, a receptor must be multidentate (i.e., it should possess several interaction points, strategically placed within its molecular framework) and rigid. Rigidity is typically achieved by giving to the receptor a cyclic shape or, better, that of a cage. It is not accidental that seminal papers of anion coordination chemistry involved hexammonium[3] and tetraalkylammonium polycyclic receptors,[4] providing ellipsoidal and spherical cavities, respectively. However, the formation of cage-like receptors is not straightforward and may require complicated and costly multistep syntheses. We have recently shown that transition metals can be conveniently used to convert quantitatively the easily accessible podands into cages, as illustrated in Scheme 1.[5]

In particular, three arms, each made by an imidazolium fragment linked to a bpy subunit, were appended to a 1,3,5-triethylbenzene platform. Then, on reaction with an iron(II) salt, the three bpy subunits coordinate the metal center to give the $[Fe^{II}(\mathbf{1})]^{5+}$ complex, which provides a tricationic cavity for anion inclusion, as illustrated in Scheme 1. Crystallographic evidence was given for the inclusion

* To whom correspondence should be addressed. E-mail: luigi.fabbrizzi@unipv.it.
[†] Dipartimento di Chimica Generale.
[‡] Centro Grandi Strumenti.
[§] Sezione INSTM.
[⊥] Present address: UMR 8601, Université Paris Descartes, 45 Rue des Saints Pères, 75006 Paris, France.

(1) Bowman-James, K. *Acc. Chem. Res.* **2005**, *38*, 671–678.
(2) (a) *Supramolecular chemistry of anions*; Bianchi, A., Bowman-James, K., García-España, E., Eds.; Wiley-VCH: New York, 1997; (b) Schmidtchen, F. P.; Berger, M. *Chem. Rev.* **1997**, *97*, 1609–1646. (c) Snowden, T. S.; Anslyn, E. V. *Curr. Opin. Chem. Biol.* **1999**, *3*, 740–746. (d) Martínez, Máñez; Sancenŏn, F. *Chem. Rev* **2003**, *103*, 4419–4476. (e) Gale, P. A. *Coord. Chem. Rev.* **2003**, *240*, 191–221. (f) Beer, P. D.; Gale, P. A. *Angew. Chem., Int. Ed.* **2001**, *40*, 486. (g) Amendola, V.; Esteban-Gomez, D.; Fabbrizzi, L.; Licchelli, M. *Acc. Chem. Res.* **2006**, *39*, 343–353. (h) Gale, P. A. *Acc. Chem. Res.* **2006**, *39*, 465–475. (i) Sessler, J. L.; Gale, P. A.; Cho, W.-S. Anion Receptor Chemistry. In *Monographs in Supramolecular Chemistry*; Stoddart, J. F., Ed.; Royal Society of Chemistry: Cambridge, 2006. (l) Amendola, V.; Bonizzoni, M.; Esteban-Gómez, D.; Fabbrizzi, L.; Licchelli, M.; Sancenón, F.; Taglietti, A. *Coord. Chem. Rev.* **2006**, *250*, 1451–1470. (m) Steed, J. W. *Chem. Commun.* **2006**, 2637–2649.
(3) Graf, E.; Lehn, J.-M. *J. Am. Chem. Soc.* **1976**, *98*, 6403–6405.
(4) Schmidtchen, F. P. *Angew. Chem., Int. Ed. Engl.* **1977**, *16*, 720.
(5) Amendola, V.; Boiocchi, M.; Colasson, B.; Fabbrizzi, L.; Rodriguez-Douton, M.-J.; Ugozzoli, F. *Angew. Chem., Int. Ed.* **2006**, *45*, 6920–6924.

10.1021/ic800099j CCC: $40.75
Published on Web 04/04/2008

Scheme 1. Formation of the Metal Complex and Anion Receptor $[M^{II}(\mathbf{1})]^{5+}$ (M = Fe, Co)

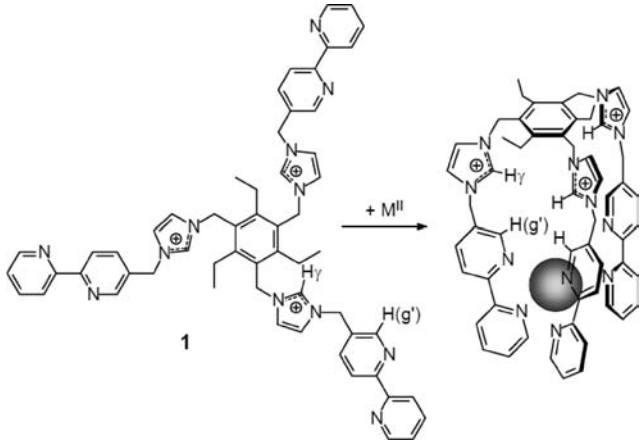

complexes of bromide and of azide.[5] In particular, it was observed that the cavity donates three H-bonds from the imidazolium C−Hγ fragments and three further H-bonds from the C−H(g′) fragments of the bpy subunits, which have been activated through metal coordination. Thus, the receptor provides the anion a six-coordinating H-bond donor set, according to a slightly distorted trigonal prismatic geometry. Fe^{II} was chosen because it forms very stable low-spin octahedral complexes with polypyridines, from both a thermodynamic and a kinetic point of view. Sensing of anion inclusion was provided by the shift of Hγ and H(g′) protons in the ^{1}H NMR spectra or by modification of the UV spectra pertinent to $\pi-\pi^*$ transition within the bpy subunits.

We wished to replace Fe^{II} with a redox active transition metal center, thus capable to signal anion inclusion through a variation of the electrochemical response. Fe^{II} itself undergoes a reversible one-electron oxidation within the $(bpy)_3$ donor set, but the potential of the Fe^{III}/Fe^{II} couple is quite high and close to that associated to the oxidation of most anions, hence causing overlapping of the voltammetric signals. Thus, we considered the Co^{II} ion as a locking metal, which gives a stable $[Co(bpy)_3]^{2+}$ complex and whose Co^{III}/Co^{II} potential is low enough for not interfering with that associated to the oxidation of most inorganic anions. We report here an investigation on the $[Co^{II}(\mathbf{1})]^{5+}$ complex, with special reference to anion inclusion and oxidation behavior. The crystal and molecular structure of the $[Co^{II}(\mathbf{1})]^{5+}$ complex containing an encapsulated water molecule is described. The synthesis of the Co^{II} complex with an analogous tripodal system in which imidazolium-bpy arms have been appended to a 1,3,5-benzene platform has been recently reported, but no mention has been made on its electrochemical response to anion binding.[6]

The $[Co^{II}(\mathbf{1})]^{5+}$ complex investigated here is a further representative of the family of redox responsive anion receptors (or electrochemical anion sensors). That is, conjugate systems in which a moiety suitable for selective anion interaction (either neutral, e.g., amides, ureas, or positively charged, e.g., guanidinium, imidazolium) is linked to a redox active fragment.[7] The by far most used redox active fragment in the design of electrochemical anion sensors is ferrocene (Fc),[8] whose oxidation to ferrocenium (Fc^+) enhances the intensity of the receptor-anion interaction through an attractive electrostatic effect, while the Fc^+/Fc couple potential is shifted to more negative values, following anion addition. The intensity of the electrostatic effect and the magnitude of ΔE signal (i.e., the difference of the potential before and after anion addition) are related to the distance between the interaction site and the redox subunit: the smaller the distance, the larger ΔE. Other redox active fragments providing a 0/+1 change of the electrical charge (and consequent switching on of binding tendencies toward the anion) include bis-dithiocarbamate Cu^{II} complexes (based on the Cu^{II}/Cu^{III} couple within a doubly negative donor set)[9] and tetra-thiafulvalene.[10] The cobaltocenium subunit, which was the first metallorganic redox active fragment used in the design of the electrochemical sensor for anions,[11] operates through the +1/0 electrical charge decrease, to which a reduction of anion binding tendencies is associated. The $[Ru^{II}(bpy)_3]^{2+}$ subunit has been used as a signaling subunit in a large variety of anion sensors, essentially in view of its unique photophysical properties.[12] Nevertheless, the complex undergoes fully reversible one-electron oxidation to the Ru^{III} form, thus providing a +2/+3 electrical charge increase. However, the potential of the $[Ru^{III}(bpy)_3]^{3+}/[Ru^{II}(bpy)_3]^{2+}$ couple is rather positive, and the metal centered oxidation may compete with that of most inorganic anions, even displaying moderate reducing tendencies. In fact, anion sensors containing the $[Ru^{II}(bpy)_3]^{2+}$ fragment have been electrochemically investigated for redox changes involving the bpy ligands (with the electron going, on reduction, onto ligand centered π^* molecular orbitals), which provide a decrease of the receptor's electrical charge and the switching off of anion binding tendencies. The system investigated here operates through a metal centered +2/+3 couple, which, taking into account the charge provided by the receptor moiety, results in a +5/+6 overall change. Significant voltammetric responses have been obtained even in aqueous media.

Experimental Section

Materials and Methods. $[\mathbf{1}](PF_6)_3$ was prepared as previously described.[5] Polarographic grade MeCN was used in spectrophotometric and electrochemical studies. Electrochemical experiments

(6) Sato, K.; Sadamitsu, Y.; Arai, S.; Yamagishi, T. *Tetrahedron Lett.* **2007**, *48*, 1493–1496.

(7) Beer, P. D.; Hayes, E. J. *Coord. Chem. Rev.* **2003**, *240*, 167–189.

(8) (a) Beer, P. D.; Chen, G. Z.; Goulden, A. J.; Graydon, A. R.; Stokes, S. E.; Wear, T. *Chem. Commun.* **1993**, 1834–1836. (b) Beer, P. D.; Graydon, A. R.; Johnson, A. O. M.; Smith, D. K. *Inorg. Chem.* **1997**, *36*, 2112–2118. (c) Abouderbala, L. O.; Warwick, J.; Belcher, W. J.; Boutelle, M. G.; Cragg, P. J.; Steed, J. W.; Turner, D. R.; Wallace, K. J. *Proc. Natl. Acad. Sci. U. S. A.* **2002**, *99*, 5001–5006.

(9) Beer, P. D.; Berry, N.; Fox, O. D.; Padilla-Tosta, M. E.; Patell, S.; Drew, M. G. B. *Chem. Commun.* **2001**, 199–200.

(10) Nielsen, K. A.; Jeppesen, J. O.; Levillain, E.; Becher, J. *Angew. Chem., Int. Ed.* **2003**, *42*, 187–191.

(11) Beer, P. D.; Keefe, A. D. *J. Organomet. Chem.* **1989**, *375*, C40-C42.

(12) (a) Szemes, F.; Hesek, F. D.; Chen, Z.; Dent, S.; Drew, M. G. B.; Goulden, A. J.; Graydon, A. R.; Grieve, A.; Mortimer, R. J.; Wear, T.; Weightman, J. S.; Beer, P. D. *Inorg. Chem.* **1996**, *35*, 5868–5879. (b) Beer, P. D.; Dent, S. W.; Wear, T. *J. Chem. Soc., Dalton Trans.* **1996**, 2341–2346.

(voltammetry and controlled potential coulometry) were performed with a BAS 100B/W electrochemical workstation. In voltammetric studies (in MeCN and aqueous MeCN solutions 0.05 M in $[Bu_4N]PF_6$), the working electrode was a platinum microsphere and the counter electrode a platinum wire. A Ag/AgCl electrode was used as pseudo reference and was calibrated versus ferrocene as an internal standard. The measured potentials were referred to the Fc^+/Fc couple (425 mV vs SCE, in CH_3CN). CPC experiments were performed by using a platinum gauze as a working electrode and a platinum coil as a counter electrode. The counter electrode compartment was separated from the working compartment by a glass frit. All compartments were filled with a MeCN solution 0.05 M in $[Bu_4N]PF_6$. The reference electrode was a Ag/AgCl electrode calibrated versus Fc^+/Fc through cyclic voltammetry (CV) experiments prior to the CPC. UV–vis spectra were recorded on a Varian CARY 100 spectrophotometer, with a quartz cuvette (path length: 0.1–1.0 cm). In the titrations with anions, UV–vis spectra of the samples were recorded after the addition of aliquots of an alkylammonium salt solution of the envisaged anion ($[BnBu_3N]^+$ for Cl^-, $([Bu_4N]^+$ for other anions). ^1H NMR spectra were obtained on a Bruker AVANCE 400 spectrometer (400 MHz) operating at 9.37 T.

X-ray Crystallographic Studies. Crystals of $[Co^{II}(\mathbf{1})\cdots H_2O]Cl(PF_6)_4\cdot 2MeCN$ suitable for X-ray diffraction studies were obtained from evaporation of a MeCN solution containing equimolar amounts of $CoCl_2.6H_2O$ and $[\mathbf{1}](PF_6)_3$. X-ray diffraction experiments on the $[Co^{II}(\mathbf{1})\cdots H_2O]Cl(PF_6)_4\cdot 2MeCN$ complex salt were performed at ambient temperature on a Bruker-Axs Smart-Apex CCD-based diffractometer. Single crystals were unstable outside the solution in which they form, and to prevent decay, diffraction data were collected with the crystal placed in a closed glass capillary containing a bit amount of mother liquor. Omega rotation frames (scan width 0.3°, scan time 40 s., sample-to-detector distance 6 cm) were processed with the SAINT software (Bruker-Axs Inc.), and intensities were corrected for Lorentz and polarization effects. Absorption effects were analytically evaluated by the SADABS software,[13] and correction was applied to the data (0.76 and 0.84 min. and max. transmission factor). Crystal data for the $[Co^{II}(\mathbf{1})\cdots H_2O]Cl(PF_6)_4\cdot 2MeCN$ complex salt: $C_{61}H_{65}ClCoF_{24}N_{14}OP_4$, $M_r = 1684.53$, $T = 293$ K, crystal dimensions $0.60 \times 0.50 \times 0.30$ mm^3, triclinic, $P\bar{1}$ (No. 2), $a = 11.294(1)$, $b = 15.209(2)$, $c = 25.188(1)$ Å, $\alpha = 79.77(1)$, $\beta = 88.13(1)$, $\gamma = 85.28(1)$, $V = 4242.5(7)$ Å^3, $Z = 2$, $\rho_{calcd} = 1.319$, $F(000) = 1714$, $\mu = 0.406$ mm^{-1}, Mo Kα X-radiation ($\lambda = 0.7107$ Å), $2\theta_{max} = 50°$, 28707 measured reflections, 14555 independent reflections ($R_{int} = 0.058$), 7247 strong reflections [$Io > 2\sigma(Io)$], 957 refined parameters, $R1 = 0.133$ (strong data) and 0.208 (all data), $wR2 = 0.370$ (strong data) and 0.410 (all data), GOF = 1.332, 1.06 and −0.89 max. and min. residual electron density.

The crystal structure was solved by direct method (SIR-97)[14] and refined by full-matrix least-squares procedures on F^2 using all reflections (SHELXL-97).[15] All non-hydrogen atoms were refined with anisotropic temperature factors; hydrogen atoms belonging to the $[Co^{II}(\mathbf{1})]^{5+}$ cationic receptor were placed using the appropriate AFIX instructions. The analysis of the final ΔF map did not allow to localize the position of the H atoms of the water molecules; therefore, the water protons have been placed at the calculated positions along the two lines that connect the O(1w) atom ant the N atom of the two acetonitrile groups.

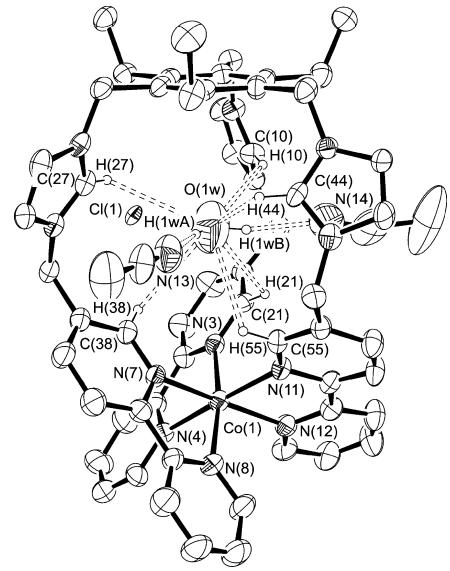

Figure 1. ORTEP view of the structure of $[Co^{II}(\mathbf{1})\cdots H_2O]Cl(PF_6)_4\cdot 2MeCN$ complex salt (thermal ellipsoids are drawn at the 30% probability level; PF_6 counterions have been omitted for clarity). Atom names are only reported for the chlorine anion, for the nitrogen atoms bonded to the metal centre, and for atoms involved in hydrogen bond interactions (drawn as dashed lines).

Results and Discussion

1. Syntheses and Structure of the $[Co^{II}(\mathbf{1})\cdots H_2O]Cl(PF_6)_4\cdot 2MeCN$ Complex Salt. On reaction of $CoCl_2\cdot 6H_2O$ with an equivalent amount of $[\mathbf{1}](PF_6)_3$ in MeCN solution, a yellow crystalline solid of formula $Co^{II}(\mathbf{1})Cl(PF_6)_4\cdot H_2O\cdot 2MeCN$ was obtained. The crystal and molecular structure of the cationic complex were determined by means of X-ray diffraction analysis, an ORTEP (Oak Ridge thermal ellipsoid plot) view of which is shown in Figure 1.

On the basis of the structural study, the salt should be described by the formula: $[Co^{II}(\mathbf{1})\cdots H_2O]Cl(PF_6)_4\cdot 2MeCN$. In fact, in full contrast to what is observed in the analogous $[Fe^{II}(\mathbf{1})\cdots Br](PF_6)_4\cdot 2H_2O\cdot MeCN$ complex salt, the cavity of the Co^{II} derivative does not include a halide ion but a water molecule. In particular, the oxygen atom of the water molecule receives from the receptor *six* H-bonds, *three* from the imidazolium C−Hγ fragments (mean O···H distance 2.91(2) Å) and *three* from the C−H(g′) fragments of the metal bound bpy subunits (mean O···H distance 3.02(2) Å). The oxygen acceptor atom is placed within a slightly distorted trigonal prism having at the corners the six hydrogen atoms, with a twist angle $\theta = 5.8(2)°$ (notice that for a regular trigonal prism $\theta = 0°$, for an octahedron $\theta = 60°$). The oxygen acceptor atom is not significantly displaced from the best line that connects the 1,3,5-trialkylbenzene cap and the metal center and is placed 3.71(2) Å from the centroid of the benzene moiety and 4.61(2) Å from the metal center. Geometrical features of the H-bond coordination are illustrated in Figure 2.

(13) Sheldrick, G. M. *SADABS: Siemens Area Detector Absorption Correction Program*; University of Göttingen: Göttingen, Germany, 1996.
(14) Altomare, A.; Burla, M. C.; Camalli, M.; Cascarano, G. L.; Giacovazzo, C.; Guagliardi, A.; Moliterni, A. G. G.; Polidori, G.; Spagna, R. *J. Appl. Crystallogr.* **1999**, *32*, 115–119.
(15) Sheldrick, G. M. *SHELX97: Programs for Crystal Structure Analysis*; University of Göttingen: Göttingen, Germany, 1997.

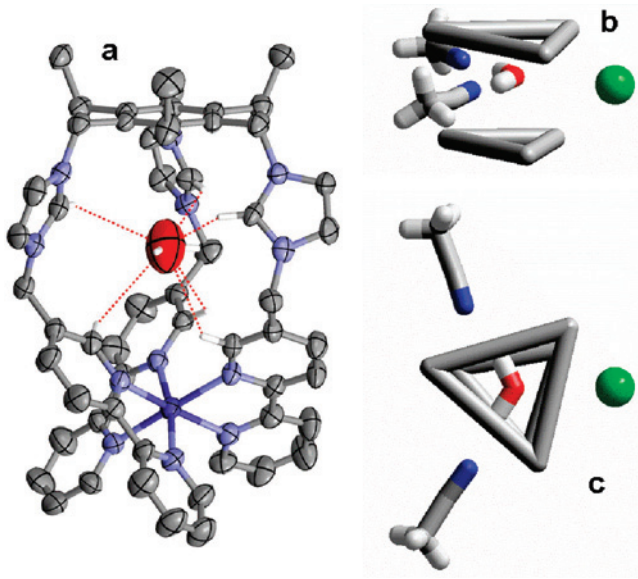

Figure 2. H-bond coordination to the oxygen atom of the water molecule included in the cavity of the $[Co^{II}(\mathbf{1})]^{5+}$ complex; (a) the oxygen acceptor atom receives six H-bonds from the imidazolium and bpy C−H fragments; (b, c) the water molecule is placed inside a slightly distorted trigonal prism having at its corners six hydrogen atoms and donates H-bonds to two close MeCN molecules. The upper triangle refers to the hydrogen atoms from the imidazolium subunits. The green sphere is a chloride ion.

Table 1. Features of the H-Bond Interactions in the $[Co^{II}(\mathbf{1})\cdots H_2O]Cl(PF_6)_4\cdot 2MeCN$ Complex Salt

donor group	D···A, Å	H···A, Å	D−H···A,°	acceptor atom
C(10)−H(10)	3.47(2)	2.80(2)	130.6(6)	O(1w)
C(21)−H(21)	3.48(2)	3.03(2)	112.3(7)	O(1w)
C(27)−H(27)	3.43(2)	2.89(2)	118.1(6)	O(1w)
C(38)−H(38)	3.42(2)	2.93(2)	114.6(7)	O(1w)
C(44)−H(44)	3.64(2)	3.03(2)	124.5(7)	O(1w)
C(55)−H(55)	3.54(2)	3.10(2)	110.5(6)	O(1w)
O(1w)−H(1wA)	3.10(2)	2.20(2) Å	172.4(8)	N(13)
O(1w)−H(1wB)	3.00(2) Å	2.10(2) Å	169.8(9)	N(14)

Water can also behave as a H-bond donor and, in this particular case, it exerts hydrogen bonding interactions with two MeCN molecules located immediately outside of the tris-imidazolium cavity, as illustrated in Figure 2b,c. In particular, the two acetonitrile molecules are placed in two of the three interspaces between the three imidazolium arms of the same receptor moiety. Features of all hydrogen bonding interactions involving the water molecule are reported in Table 1.

In the third available site close to the cavity, there is one chloride ion, which does not interact with the encapsulated water molecule, but that, being placed between symmetrically related $[Co^{II}(\mathbf{1})\cdots H_2O]^{5+}$ cationic complexes, favors the formation of molecular chains extending along the *a* axis in the crystal.

The geometrical features of the Co^{II} metal center are reported in Table 2. The metal is octahedrally coordinated by six nitrogen atoms of three bpy moieties, which are placed on three planes forming dihedral angles of 76.3(1), 83.0(1), and 86.0(1)°. The observed Co−N bond distances, with mean value of 2.136(8) Å, are similar to those observed for discrete high-spin $Co^{II}(bpy)_3^{2+}$ octahedral complexes (2.126 Å)[16] and are significantly longer than those observed for low-spin Co^{III} derivatives (1.934 Å).[16]

Table 2. Bond Distances (Å) and Bond Angles (°) around the Metal Center in the $[Co^{II}(\mathbf{1})\cdots H_2O]Cl(PF_6)_4\cdot 2MeCN$ Complex Salt

Co(1)−N(3)	2.132(7)	N(4)−Co(1)−N(7)	88.4(3)
Co(1)−N(4)	2.160(8)	N(4)−Co(1)−N(8)	93.4(3)
Co(1)−N(7)	2.127(7)	N(4)−Co(1)−N(11)	174.4(3)
Co(1)−N(8)	2.116(8)	N(4)−Co(1)−N(12)	97.9(3)
Co(1)−N(11)	2.141(7)	N(7)−Co(1)−N(8)	77.1(3)
Co(1)−N(12)	2.142(7)	N(7)−Co(1)−N(11)	96.9(3)
N(3)−Co(1)−N(4)	77.8(3)	N(7)−Co(1)−N(12)	172.8(3)
N(3)−Co(1)−N(7)	99.7(3)	N(8)−Co(1)−N(11)	89.7(3)
N(3)−Co(1)−N(8)	170.8(3)	N(8)−Co(1)−N(12)	99.0(3)
N(3)−Co(1)−N(11)	99.3(3)	N(11)−Co(1)−N(12)	77.0(3)
N(3)−Co(1)−N(12)	85.0(3)		

Quite interestingly, the structural features of the $[Co^{II}(\mathbf{1})\cdots H_2O]^{5+}$ complex are rather similar to those observed for the $[Fe^{II}(\mathbf{1})\cdots Br]^{4+}$ species. The main geometrical differences are related to the high-spin Co^{II}−N bond distances, which are distinctly longer than that observed for the low-spin Fe^{II} analogue (1.973(8) Å). The longer Co^{II}−N distance makes the base of the tripod larger, thus inducing a shortening of the axis of the cage. Actually, the distance between the centroid of the 1,3,5-trialkylbenzene cap and the metal center is 8.32(3) Å in $[Co^{II}(\mathbf{1})\cdots H_2O]^{5+}$ and 8.56(2) Å in $[Fe^{II}(\mathbf{1})\cdots Br]^{4+}$.

It may seem surprising that the $[Co^{II}(\mathbf{1})]^{5+}$ receptor includes a water molecule rather than a chloride ion, but this probably depends upon effects related to the solid state arrangement. First, the encapsulated water behaves as a H-bond donor and establishes additional hydrogen bonding interactions with two MeCN molecules. Then, the chloride ion, staying outside of the cavity, can promote the formation of molecular chains which extend along the *a* crystalline axis. Studies in solution (vide infra) will demonstrate the high tendency of $[Co^{II}(\mathbf{1})]^{5+}$ to include anions into its tris-imidazolium cavity, even in an aqueous medium.

2. $[Co^{II}(\mathbf{1})]^{5+}$ Complex in Solution: Stability and Magnetic Properties. The formation of the $[Co^{II}(\mathbf{1})]^{5+}$ complex in MeCN has been investigated through a spectrophotometric titration. Figure 3 shows the family of spectra recorded over the course of the titration of a 10^{-4} M solution of $[\mathbf{1}](PF_6)_3$ with a standard solution of $Co^{II}(CF_3SO_3)_2$. On Co^{II} addition, the $\pi-\pi^*$ band centered on the bpy moieties is distinctly red-shifted and split into two bands, as a consequence of metal coordination. The titration profile shown in the inset indicates the formation of a complex of 1:1 stoichiometry, that is, $[Co^{II}(\mathbf{1})]^{5+}$. However, lack of curvature at the equivalent point prevents any determination of the constant of the complexation equilibrium, whose value can only be estimated as >10.[6]

Octahedral d^7 complexes can exhibit either high-spin ($t_{2g}^5e_g^2$) or low-spin ($t_{2g}^6e_g^1$) configuration, depending upon the strength of the ligand field. Both configurations are paramagnetic and can be discriminated by the magnetic moment. d^7 $[Co^{II}(bpy)_3]^{2+}$ complexes normally have a high-spin ground-state and a low-lying low-spin excited state. The Evans' method[17] for the magnetic moment determination confirmed the high-spin configuration for both the $[Co^{II}(\mathbf{1})]^{5+}$

(16) The Cambridge Structural Database; a quarter of a million crystal structures and rising, Allen, F. H. *Acta Crystallogr.* **2002**, *B58*, 380–388.

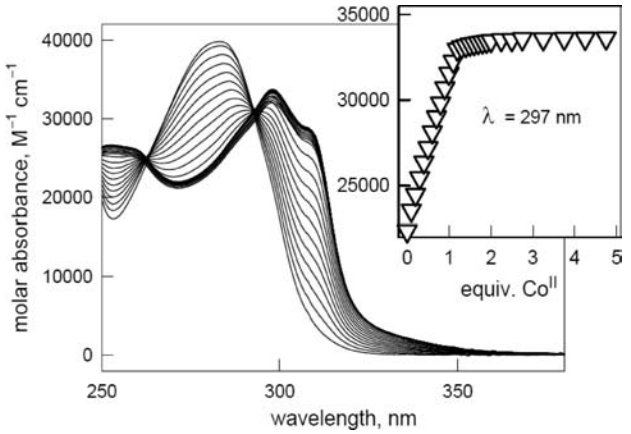

Figure 3. Spectra recorded over the course of the titration of a 10^{-4} M solution of [**1**](PF$_6$)$_3$ with a standard solution of Co^{II}(CF$_3$SO$_3$)$_2$ in MeCN. Inset: titration profile at 297 nm, which demonstrates the formation of the [Co^{II}(**1**)]$^{5+}$ complex.

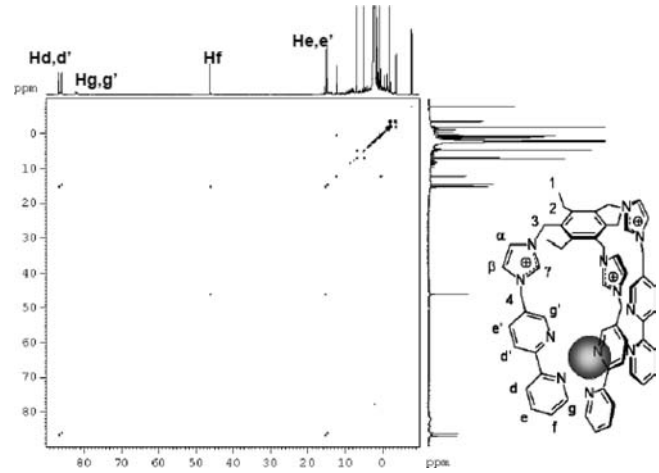

Figure 4. ^{1}H−^{1}H DQF-COSY spectrum of a 7×10^{-3} M solution of [Co^{II}(**1**)]$^{5+}$ in CD$_3$CN.

derivative ($\mu_{eff} = 4.2\ \mu_B$) and the parent complex [Co(bpy)$_3$](CF$_3$SO$_3$)$_2$ (4.1 μ_B). The comparison with the calculated $\mu_{S-O} = 3.9\ \mu_B$ for the spin-only magnetic moment value indicates a small but not negligible orbital contribution. Evans' measurements were performed on 7.0×10^{-3} M solutions of the complexes in CD$_3$CN at 295 K. For magnetic moment (μ_{eff}) calculations, the Curie eq 1 was applied.

$$\mu_{eff} = 797.74(\chi_M T)^{0.5} \quad (1)$$

The short electronic relaxation time for the [Co^{II}(**1**)]$^{5+}$ complex allowed an easy recording and interpretation of the ^{1}H NMR spectrum (see Supporting Information, Figure S1).[18] The unpaired electron causes large shifts in the proton resonances with only a moderate broadening of the peaks. The majority of the peaks present line widths varying from 10 to 30 Hz except for the peak at 82 ppm, which is significantly broader (300 Hz). *J*-coupling was observed only for aliphatic protons and for those of the imidazolium group, whereas the other aromatic signals appeared as broad singlets. The complete assignment could be obtained through COSY studies.

The 400 MHz ^{1}H−^{1}H DQF-COSY spectrum of the [Co^{II}(**1**)]$^{5+}$ complex solution is shown in Figure 4. The paramagnetic pattern can be accounted for by assuming the presence of both unpaired electrons in e_g and t_{2g} orbitals, with orbital contributions at the ground state. As a result, both the contact (direct and through spin polarization) and the dipolar contributions to the paramagnetic shifts are present. For the groups directly bound to the metal ion, the direct contribution dominates, giving rise to a global downfield shift of bpy protons signals. The most shifted peaks are assigned to H(d) and H(d′) (86.9 and 86.3 ppm, respectively), showing cross peaks in the COSY spectrum with H(e) and H(e′) (at δ 15.1 ppm and 14.9 ppm, respectively).

The relatively high broadness of the signals in the range δ 80.0–85.0 ppm does not allow one to obtain information on the multiplicity and to observe any detectable cross peak. The signals can be intuitively attributed to H(g) and H(g′), for which the closeness to the paramagnetic center induces strong relaxation. The peak at δ 46.1 ppm can be unambiguously attributed to H(f), presenting cross peaks with both H(e) and H(d). The pseudocontact shift dominates in the case of the protons of groups not directly bound to the metal ion, and the paramagnetic center can induce also upfield shifts through its magnetic field anisotropy. The imidazolium protons Hα and Hβ show two peaks at δ 4.9 ppm and 5.2 ppm, whereas Hγ is dramatically upfield shifted at −7.9 ppm (see Supporting Information, Figure S2). The protons of the aliphatic groups of the [Co^{II}(**1**)]$^{5+}$ complex are all upfield shifted (besides one of the methylenic proton H(4); in particular, the multiplet at −3.5 ppm can be assigned to H(2), whereas the broad singlet at −2.0 ppm is attributed to H(1). Another anisotropic effect is the strong splitting of the methylenic protons H(4) in two broad doublets at δ 12.3 ppm and 0.4 ppm. Interestingly, the isotropic shift for the two protons has opposite value; this is in agreement with both a rigid coordination of the ligand, which does not allow the averaging of the chemical shift, and with a disposition of the nuclei at opposite sites of the shielding cone generated by the paramagnetic metal ion (i.e., close to the magic angle). A similar but smaller effect is observed for H(3), split in two sharp doublets at 0.6 and 0.8 ppm. It should be noted that this strong anisotropic effect is consistent with the high-spin ($t_{2g}^5 e_g^2$) configuration of the complex and, in particular, with the possibility that the unpaired electron circulates

(17) Evans, D. F. *J. Chem. Soc.* **1959**, 2003–2005. (a) Sur, S. K. *J. Magn. Reson.* **1989**, *82*, 169–173.
(18) Bertini, I.; Luchinat, C. NMR of paramagnetic substances. *Coord. Chem. Rev.*, **1996**, Vol. *150*.
(19) The supporting electrolyte (0.05 M [Bu$_4$N]PF$_6$) exerts a dramatic effect on the stability of the [Co^{II}(**1**)]$^{5+}$···Cl]$^{4+}$ inclusion complex. In fact, in the absence of electrolyte, significant spectral modifications were observed on titration with chloride; on non-linear least-squares treatment of spectrophotometric titration data, a log $K^{II} = 3.9 \pm 0.1$ was obtained. This value coincides with that previously determined in the case of the analogous [Fe^{II}(**1**)]$^{5+}$···Cl]$^{4+}$ inclusion complex in MeCN/H$_2$O 4:1 v/v, log $K^{II} = 3.9 \pm 0.1$.[5] Background effect on *K* values has probably to be ascribed to the competition for the receptor of the anion of the electrolyte (PF_6^-, in this case), which is present in a 1000-fold excess and more. Moreover, the competition by water for the cavity of the Co^{II} containing receptor should also be taken into account, as anticipated by the structure of the [Co^{II}(**1**)···H$_2$O]Cl(PF$_6$)$_4$·2MeCN salt, whose crystals had been grown in wet MeCN.

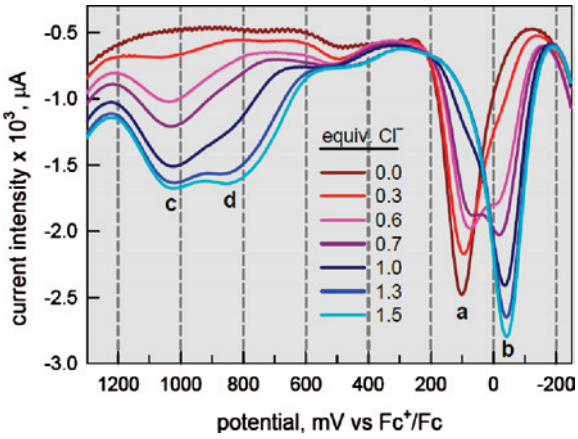

Figure 5. DPV profiles obtained at a platinum working electrode over the course of the titration of a MeCN solution 7×10^{-4} M of $[Co^{II}(\mathbf{1})]^{5+}$ and 0.05 M in $[Bu_4N]PF_6$ with a standard solution of $[BnEt_3N]Cl$. Oxidation scan from −200 mV to 1200 mV vs Fc^+/Fc.

in the t_{2g} orbitals, together with small distortion from a perfect octahedral geometry.

3. Co^{III}/Co^{II} Redox Couple: Effect of Anion Inclusion. Voltammetric studies were carried out on a MeCN solution 7×10^{-4} M in $[Co^{II}(\mathbf{1})]^{5+}$ (obtained by mixing equimolar amounts of $[\mathbf{1}](PF_6)_3$ and $Co^{II}(CF_3SO_3)_2$) made 0.05 M in $[Bu_4N]PF_6$. Figure 5 shows the Differential Pulse Voltammetry (DPV) profile obtained at a platinum microsphere working electrode over the −200 mV to 1200 mV oxidation scan (vs the Fc^+/Fc reference couple). A peak at 100 mV was observed, corresponding to the oxidation half-reaction: $[Co^{II}(\mathbf{1})]^{5+} \rightleftharpoons [Co^{III}(\mathbf{1})]^{6+} + e^-$ (brown line, peak **a**). It should be noticed that this value is slightly more positive than that measured for the model $[Co^{II}(bpy)_3]_{2+}$ complex, determined in the same conditions (30 mV vs Fc^+/Fc). It is suggested that the more difficult oxidation to the Co^{III} state in the $[Co^{II}(\mathbf{1})]^{5+}$ complex results from the electrostatic repulsions exerted by the proximate tris-imidazolium cage.

Then, the solution was titrated with a MeCN solution 5×10^{-2} M in $[BnBu_3N]Cl$. On chloride addition, the intensity of peak **a** decreased, while a new peak, **b**, developed at a more cathodic potential. The new peak must be ascribed to the oxidation of the $[Co^{II}(\mathbf{1})]^{5+}$ complex including a Cl^- ion, that is, to the half-reaction: $[Co^{II}(\mathbf{1})\cdots Cl]^{5+} \rightleftharpoons [Co^{III}(\mathbf{1})\cdots Cl]^{6+} + e^-$. At the same time, a new peak grew at about 1050 mV, **c**, which should be assigned to the oxidation of the chloride ion inside the tris-imidazolium cage, half-reaction $[Co^{III}(\mathbf{1})\cdots Cl]^{6+} \rightleftarrows [Co^{III}(\mathbf{1})]^{6+} + Cl\cdot + e^-$. After the addition of 1 equiv of chloride, a new peak, **d**, developed: this peak results from the oxidation of Cl^- in excess, dispersed in the solution (half-reaction: $Cl^- \rightleftharpoons Cl\cdot + e^-$). Two main points should be noted: (i) on chloride addition the Co^{III}/Co^{II} potential becomes more negative, that is, the Co^{III} state is stabilized with respect to Co^{II}; (ii) encapsulation by a triply positively charged cage makes the potential of the $Cl\cdot/Cl^-$ couple more positive, that is, it leaves the anion more resistant to the oxidation.

A similar behavior was observed over the course of the titration of a MeCN solution 7×10^{-4} M in $[Co^{II}(\mathbf{1})]^{5+}$ with

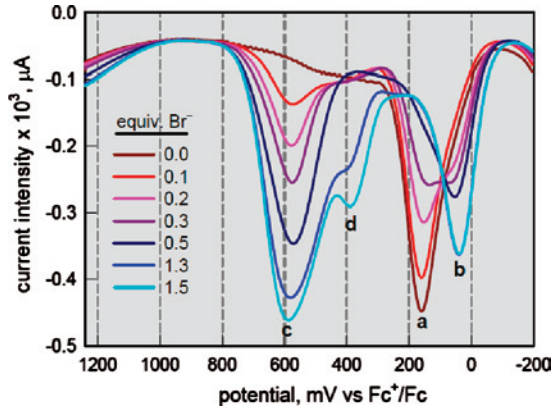

Figure 6. DPV profiles obtained at a platinum working electrode over the course of the titration of a MeCN solution 7×10^{-4} M of $[Co^{II}(\mathbf{1})]^{5+}$ and 0.05 M in $[Bu_4N]PF_6$ with a standard solution of $[Bu_4N]Br$. Oxidation scan from −200 mV to 1200 mV vs Fc^+/Fc.

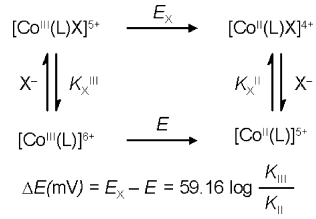

Figure 7. Thermodynamic cycle for the $[Co^{II}(\mathbf{1})]^{5+}/[Co^{III}(\mathbf{1})]^{6+}$ redox change in the presence of the anion X^-, which forms stable 1:1 complexes with the receptor in both oxidation states. K_X^{II} and K_X^{III} are the constants of the association equilibria of the receptors $[Co^{II}(\mathbf{1})]^{5+}$ and $[Co^{III}(\mathbf{1})]^{6+}$, respectively.

$[Bu_4N]Br$, whose DPV profiles are shown in Figure 6. It is observed that also in this case complex formation (i) induces a significant stabilization of the Co^{III} state and (ii) increases halide resistance to the oxidation. In particular, the voltammetric behavior illustrated in Figures 5 and 6 can be quantitatively explained on the basis of the thermodynamic cycle shown in Figure 7.

In particular, from the peak separation, $\Delta E = E_X - E$, it is possible to calculate the ratio of the association constants of the receptors in the two oxidation states: for chloride $\Delta E = 144$ mV and $\log(K^{III}/K^{II}) = 2.44$; for bromide $\Delta E = 120$ mV and $\log(K^{III}/K^{II}) = 2.03$. As reasonably expected, the receptor of higher charge, $[Co^{III}(\mathbf{1})]^{6+}$, forms more stable complexes than the receptor of lower charge, $[Co^{II}(\mathbf{1})]^{5+}$. This can be due to an intensified attractive electrostatic effect, but also to the increase of the H-bond donor properties of the C−H(g′) fragments, which have been more intensely activated by the proximate low-spin Co^{III} center.

Attempts to calculate K^{II} values failed, in view of the too high stability of the $[Co^{II}(\mathbf{1})\cdots X]^{4+}$ complexes. In this connection, Figure 8 shows the spectra obtained over the course of the titration of solution 10^{-4} M of $[Co^{II}(\mathbf{1})]^{5+}$ with $[Bu_4N]Br$. On bromide addition, the intensity of the $\pi-\pi^*$ band decreases. The titration profile shown in the inset exhibits a definite discontinuity on addition of 1 equiv. of anion, which indicates the formation of a 1:1 inclusion complex, whose association constant can be only estimated as higher than 10^6. The same behavior was observed for chloride. Noticeably, the same spectral response was observed on a MeCN solution made 0.05 M in $[Bu_4N]PF_6$, that

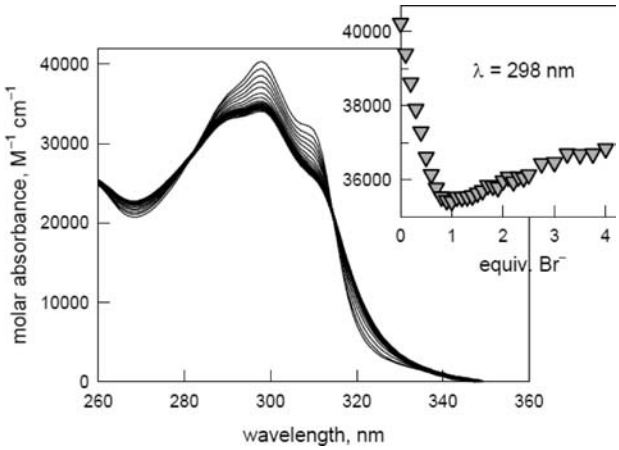

Figure 8. Spectra recorded over the course of the titration of a MeCN solution 10^{-4} M in $[Co^{II}(\mathbf{1})]^{5+}$, with a standard solution of $[Bu_4N]Br$. Inset: titration profile at 298 nm.

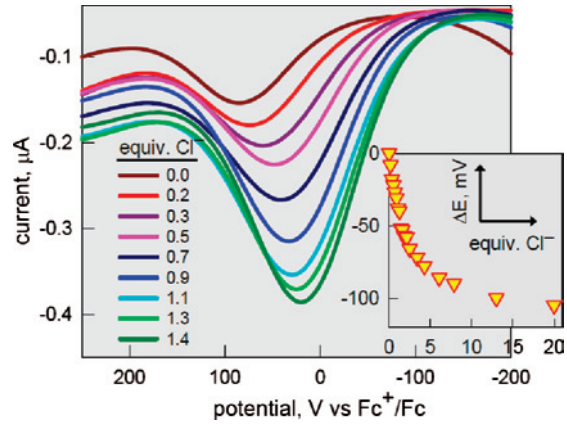

Figure 9. DPV profiles obtained at a platinum working electrode over the course of the titration of a MeCN/H_2O solution (4:1 v/v) 7×10^{-4} M of $[Co^{II}(\mathbf{1})]^{5+}$ and 0.05 M in $[Bu_4N]PF_6$ with a standard solution of $[BnBu_3N]Cl$. Oxidation scan from –200 mV to 200 mV vs Fc^+/Fc.

is, under the conditions of electrochemical studies (vide infra). Thus, also in this medium, K^{II} values must be $\geq 10^6$, for both Cl^- and Br^-. Therefore, from ΔE values, it derives that K^{III} is $\geq 10^8$ for the two halide ions.

Quite disappointingly, voltammetric studies in pure MeCN could not be extended to many other anions, in particular when they presented a distinct reducing attitude. This was the case of I^- and NCS^-, whose oxidation peaks overlapped the peaks pertinent to the oxidation of the metal center. On the other hand, the oxidation resistant anions, HSO_4^- and NO_3^-, did not cause any significant modification of the voltammetric response, even if added in large excess. NCO^- induced demetalation of $[Co^{II}(\mathbf{1})]^{5+}$ with eventual formation of $[Co^{II}(NCO)_4]^{2-}$.

At this stage, we considered that, to separate the peaks pertinent to the $[Co^{II}(\mathbf{1})]^{5+}/[Co^{III}(\mathbf{1})]^{6+}$ change from those corresponding to the oxidation of the anion, we had to move to a medium of higher polarity. In fact, a more polar medium is expected to stabilize electrically charged species with respect to species which are neutral or detain a lower electrical charge: therefore, (i) X^- will be stabilized over $X^{\bullet}$, thus making $E(X^{\bullet}/X^-)$ increase, and (ii) $[Co^{III}(\mathbf{1})]^{6+}$ will be stabilized over $[Co^{II}(\mathbf{1})]^{5+}$, thus making $E(Co^{III}/Co^{II})$ decrease. As a consequence, potentials pertinent to the oxidation of the metal center and of the anion could be conveniently separated.

Therefore, voltammetric titrations were performed in a MeCN/H_2O mixture 4:1 v/v. The large portion of water is expected to increase significantly the polar nature of the medium. Rather surprisingly, the electrochemical response was quite different from that observed in pure MeCN. In particular, on anion addition, the DPV peak associated to the $[Co^{II}(\mathbf{1})]^{5+}/[Co^{III}(\mathbf{1})]^{6+}$ oxidation process did not decrease in intensity (and no new peak grew up at a more cathodic potential), but it simply shifted toward more negative potentials. Figure 9 shows the family of voltammetric profiles obtained on titration with chloride. In particular, the oxidation peak, on anion addition, is cathodically shifted according to a saturation profile, as illustrated in the inset of Figure 9.

This solvent dependent electrochemical behavior can be interpreted by considering two distinct limiting situations.

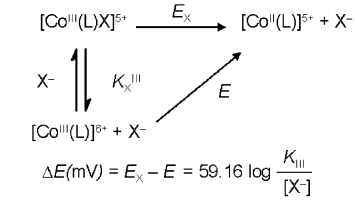

Figure 10. Thermodynamic cycle for the $[Co^{II}(\mathbf{1})]^{5+}/[Co^{III}(\mathbf{1})]^{6+}$ redox change in the presence of the anion X^-, which forms a stable 1:1 complex only with the receptor in the highest oxidation state, $[Co^{III}(\mathbf{1})]^{6+}$. K_X^{III} is the constants of the association equilibrium of the receptor $[Co^{III}(\mathbf{1})]^{6+}$ with X^-.

One situation has been already illustrated in Figure 7 and refers to the case in which both $[Co^{III}(\mathbf{1})]^{6+}$ and $[Co^{II}(\mathbf{1})]^{5+}$ form stable inclusion complexes with the anion X^-, characterized by rather high association constants K^{III} and K^{II}, respectively. In such a situation, ΔE is independent of $[X^-]$, thus remaining constant over the course of the titration. An opposite limiting situation exists, illustrated in Figure 10, in which one of the redox active receptors, that is, $[Co^{II}(\mathbf{1})]^{5+}$, does not show any detectable affinity toward X^-. Under these circumstances ΔE depends upon $[X^-]$.

It appears that the behavior in aqueous MeCN is closer to that described by the scheme of Figure 10 than by the scheme of Figure 7. To corroborate such a hypothesis, attempts were made to estimate K^{II} and K^{III} values in aqueous MeCN. As far as K^{II} is concerned, a MeCN/H_2O 4:1 v/v solution, 10^{-4} M in $[Co^{II}(\mathbf{1})]^{5+}$ and 0.05 M in $[Bu_4N]PF_6$, was titrated with chloride. However, no detectable modifications were observed in the $\pi-\pi^*$ region of the absorption spectrum even on excess chloride addition, thus indicating a value $\leq 10^2$ for K^{II}.[19] On the other hand, a log $K^{III} = 4.42 + 0.02$ value could be determined through an independent spectrophotometric titration experiment on a $[Co^{III}(\mathbf{1})]^{6+}$ solution obtained by bulk electrolysis. In particular, a controlled potential coulometry (CPC) experiment was carried out on a MeCN solution, 10^{-4} M in $[Co^{II}(\mathbf{1})]^{5+}$ and 0.05 M in $[Bu_4N]PF_6$, by setting the potential of the working electrode (a platinum gauze) at + 300 mV versus Fc^+/Fc. Over the course of the CPC experiment, the light yellow solution turned bright yellow, while substantial modifications were observed in the $\pi-\pi^*$ region of the spectrum, as shown in Figure 11. In

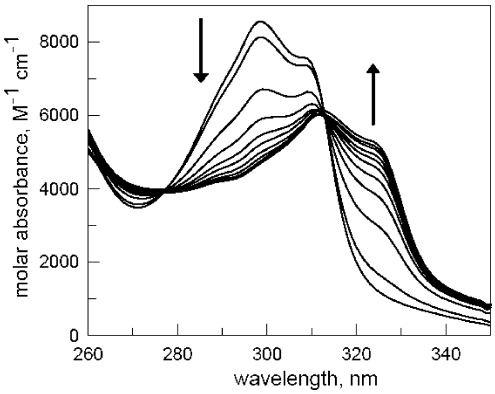

Figure 11. Spectra recorded over the course of the CPC experiment on a MeCN solution 10^{-4} M in $[Co^{II}(\mathbf{1})]^{5+}$ and 0.05 M in $[Bu_4N]PF_6$.

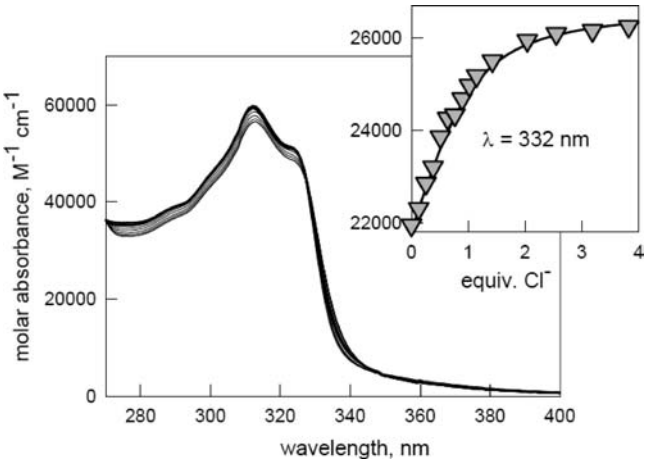

Figure 12. Spectra recorded over the course of the titration of a 4/1 MeCN/H_2O solution 7.5×10^{-5} M in $[Co^{III}(\mathbf{1})]^{6+}$ and 0.05 M in $[Bu_4N]PF_6$, with a standard solution of $[BnEt_3N]Cl$. The oxidized $[Co^{III}(\mathbf{1})]^{6+}$ complex solution was obtained by bulk electrolysis on a MeCN solution of $[Co^{II}(\mathbf{1})]^{5+}$. Inset: titration profile at 332 nm.

particular, on oxidation, a red shift of the $\pi-\pi^*$ bpy centered transitions is observed.

The passage of 1.0 ± 0.1 electrons was determined through coulometry. The electrolyzed solution, containing the $[Co^{III}(\mathbf{1})]^{6+}$ complex, was treated with water and $[Bu_4N]PF_6$ to obtain a 4/1 MeCN/H_2O solution 0.05 M in $[Bu_4N]PF_6$. Then, the aqueous MeCN solution was titrated with a standard solution of chloride. Anion addition induced small yet significant spectral modifications, as shown in Figure 12. The titration profile (see the inset of Figure 12) showed a convenient curvature at the equivalent point, and a reliable value of K^{III} could be calculated through multiwavelength nonlinear least-squares treatment of the titration data using the HyperQuad program:[20] $\log K^{III} = 4.42 + 0.02$. Thus, values of K^{III} and K^{II} indicate that the $[Co^{II}(\mathbf{1})]^{5+}/Cl^-$ system can be conveniently interpreted on the basis of the triangular scheme of Figure 10.

The voltammetric behavior of redox active receptors in the presence of an electrically charged analyte has been treated in its quantitative details in the case of the interaction of crown ethers with an appended nitrobenzene fragment with Na^+.[21] Nitrobenzene is redox active through the $-NO_2/-NO_2^-$ couple. In particular, the negatively charged receptor ($-NO_2^-$ form) showed a higher affinity toward Na^+ than the neutral receptor ($-NO_2$),[22] in a way specular to that investigated in this study.

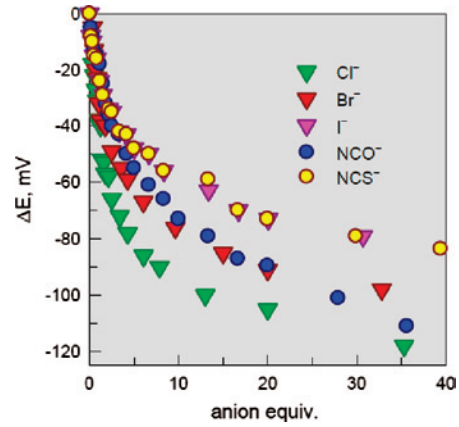

Figure 13. Titration of a MeCN/water solution (4:1 v/v) of $[Co^{II}(\mathbf{1})]^{5+}$ with halide and pseudohalides tetraalkylammonium salts. ΔE expresses the shift of the potential of the Co^{III}/Co^{II} couple induced by anion addition.

The voltammetric investigation in aqueous MeCN was successfully extended to other halide and pseudohalide anions, for which the peak associated to the Co^{III}/Co^{II} redox change resulted distinctly separated from the peaks related to anion oxidation. In all cases, a continuous cathodic shift of the potential was observed on anion addition. Pertinent profiles of the Co^{III}/Co^{II} redox couple potential are shown in the diagram in Figure 13. ΔE values at the highest investigated anion excess increase along the series: $I^- \sim NCS^- < NCO^- \sim Br^- < Cl^-$, which parallels anion tendencies to receive H-bonds. It has to be noted that in aqueous MeCN, NCO^- does not induce demetalation of the $[Co^{II}(\mathbf{1})]^{5+}$. In fact, NCO^- seems well satisfied of the interactions with water molecules and does not seek Co^{II} for complex formation.

The effect of the gradual modification of solvent polarity on the voltammetric response of the $[Co^{II}(\mathbf{1})]^{5+}/Cl^-$ system is illustrated in Figure 14. In particular, the Figure shows the DPV profiles taken on MeCN solutions 2×10^{-3} M in $[Co^{II}(\mathbf{1})]^{5+}$ and 1×10^{-3} M in Cl^-, containing varying amounts of water (from 0 to 20%; notice that the scale of the water content is not linear but refers to the following percent of H_2O: 0, 1, 2, 4, 10, 20%).

It is observed that, on water addition to the MeCN solution, the two DPV peaks, one corresponding to the $[Co^{III}(\mathbf{1})]^{6+}/[Co^{II}(\mathbf{1})]^{5+}$ couple (more anodic) and the other corresponding to the $[Co^{III}(\mathbf{1})\cdots Cl]^{5+}/[Co^{II}(\mathbf{1})\cdots Cl]^{4+}$ couple (more cathodic), approach each other to eventually coalesce in a single peak, centered at an intermediate potential. This reflects the gradual decrease of the stability of the $[Co^{II}(\mathbf{1})\cdots Cl]^{4+}$ receptor-anion complex and the smooth change from the regime described in Figure 7 to that described in Figure 10.

(20) Gans, P.; Sabatini, A; Vacca, A. *Talanta* **1996**, *43*, 1739–1753; http://www.hyperquad.co.uk.

(21) Miller, S. R.; Gustowski, D. A.; Chen, Z.-H.; Gokel, G. W.; Echegoyen, L.; Kaifer, A. E. *Anal. Chem.* **1988**, *60*, 2021–2024.

(22) (a) Kaifer, A.; Echegoyen, L.; Gustowski, D.; Goli, D. M; Gokel, G. *J. Am. Chem. Soc.* **1983**, *105*, 7168–7169. (b) Gustowski, D. A.; Echegoyen, L.; Goli, D. M.; Kaifer, A; Schultz, R. A; Gokel, G. W. *J. Am. Chem. Soc.* **1984**, *106*, 1633–1635. (c) Morgan, C. R.; Gustowski, D. A.; Cleary, T. P.; Echegoyen, L.; Gokel, G. W. *J. Org. Chem.* **1984**, *49*, 5008–4010.

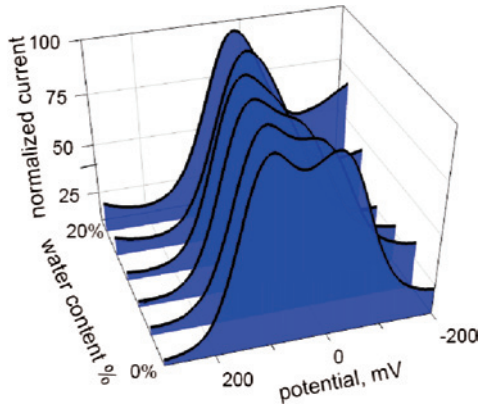

Figure 14. DPV profiles obtained over the –200 mV to 300 mV oxidation scan on MeCN solutions 2×10^{-3} M in $[Co^{II}(\mathbf{1})]^{5+}$ and 1×10^{-3} M in Cl^-, containing a varying amount of water. The scale of the axis of water content is not linear, but arbitrary; in particular, DPV profiles refer to solutions whose water content was 0, 1, 2, 4, 10, 20%. The *z* axis reports the increasing anodic current (opposite convention with respect to Figures 6 and 9).

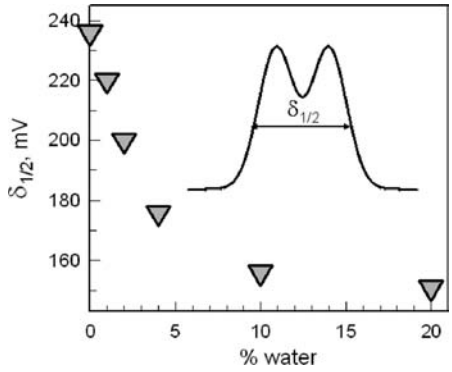

Figure 15. Effect of the water content on the DPV profile associated to the $[Co^{III}(\mathbf{1})]^{6+}/[Co^{II}(\mathbf{1})]^{5+}$ in presence of Cl^-, in aqueous MeCN; $\delta_{1/2}$ is. the distance in mV between the ascending branch of the more anodic peak and the descending branch of the more cathodic peak, at mid intensity.

The passage from one regime to another is pictorially illustrated in Figure 15. In the diagram, the $\delta_{1/2}$ parameter was considered, that is, the distance in mV between the ascending branch of the more anodic peak and the descending branch of the more cathodic peak, at mid intensity. It can be observed that important changes in the electrochemical response take place on addition of the first small amounts of water to MeCN. This suggests the occurrence of a selective interaction of the water molecules with the anion and the receptor, which leads to an early decomposition of the $[Co^{II}(\mathbf{1})\cdots Cl]^{4+}$ complex and to the passage from the regime of Figure 7 to that of Figure 10.

Conclusions

The design of redox responsive receptors for anions is a lively and challenging topic of supramolecular chemistry.[23] Most of the investigated receptors are neutral and must operate in apolar or poorly polar media to avoid the competition of the solvent for the anion. Water, in particular, has to be excluded because it would establish stronger hydrogen bonding interactions with the anion than the N−H fragments from amides, ureas, and pyrroles typically employed to build up receptors. As a consequence, neutral and lipophilic redox active fragments have to be considered as signaling units when designing the receptor. In this sense, ferrocene is an ideal component, which explains its absolute predominance as a redox fragment used in the synthesis of electrochemical anion sensors. On the other hand, receptors containing positively charged H-bond donors, like imidazolium,[24] are able to form stable anion complexes even in aqueous media, which makes them compatible with highly positively charged redox fragments like cationic transition metal complexes. In particular, this work has demonstrated that the $[Co^{II}(bpy)_3]^{2+}/[Co^{III}(bpy)_3]^{3+}$ couple, when operating within the $[\mathbf{1}]^{3+}$ system, is able to sense the different tendencies of anions to receive H-bonds in aqueous solution with significant selectivity. Studies on anion recognition and sensing are being currently carried out in a variety of solvent of different polarity (from chloform and dichloromethane to water). The studies in MeCN solutions containing varying amounts of water reported here allowed to clearly define the effect of the solvent on the appearance of the voltammetric response provided by electrochemical sensors.

Acknowledgment. The financial support of the Italian Ministry of University and Research (PRIN - Dispositivi Supramolecolari) is gratefully acknowledged.

Supporting Information Available: X-ray crystallographic files in CIF format for the $[Co^{II}(\mathbf{1})\cdots H_2O]Cl(PF_6)_4\cdot 2MeCN$ complex salt. ^1H NMR spectrum of $[Co^{II}(\mathbf{1})]^{5+}$ in CD_3CN; $^1H-^1H$ DQF-COSY spectrum of $[Co^{II}(\mathbf{1})]^{5+}$ in CD_3CN. This material is available free of charge via the Internet at http://pubs.acs.org.

IC800099J

(23) Atwood, J. L.; Steed, J. W. *Supramolecular Chemistry*; John Wiley & Sons, Ltd.: New York, 2000; Encyclopedia of Supramolecular Chemistry; Atwood, J. L., Steed, J., Eds.; Dekker: New York, 2004.
(24) Yoon, J.; Kim, S. K.; Singh, N. J.; Kim, K. S. *Chem. Soc. Rev.* **2006**, *35*, 355–360.